

Please cite this article as: C. Arkar, S. Domjan, S. Medved: Lightweight composite timber façade wall with improved thermal response, *Sustainable Cities and Society* 38 (2018) 325–332; <https://doi.org/10.1016/j.scs.2018.01.011>

NOTE: This is a PDF file of an unedited manuscript that has been accepted for publication to *Sustainable Cities and Society*. Therefore, the information contained in this manuscript may change before publication.

Lightweight composite timber façade wall with improved thermal response

Ciril Arkar*, Suzana Domjan, Sašo Medved

Laboratory for Sustainable Technologies in Buildings, Faculty of Mechanical Engineering, University of Ljubljana, Aškerčeva 6, 1000 Ljubljana, Slovenia

Abstract

For the construction of modern energy-efficient buildings, lightweight construction is becoming very popular among designers. EU legislation encourages such design, especially if wood, as a sustainable material, is used. However, lightweight building envelope construction, in general, exhibits poor dynamic thermal properties, which are particularly pronounced in prefabricated metal walls and thin wooden or composite building panels, such as door fillers or opaque parts (parapets) of prefabricated walls with the glazing of the skeleton-built buildings. The aim of this research was the development of a composite timber façade wall, which will not exceed the thickness of building elements, such as doors and windows, and will meet the requirements of energy efficiency and have improved dynamic thermal properties. The composite timber building element with a thickness of 68 mm, which includes two layers of advanced technologies: vacuum insulation panel (VIP) and phase change material (PCM), was developed and optimized. The optimization included a parametric study on VIP and PCM panels' position in the thin, lightweight building wall. The research has shown that dynamic thermal properties comparable to the heavyweight building envelope constructions (time lag of the heat wave up to 12 hours) can be achieved; moreover, the thermal transmittance is considerably reduced.

Keywords:

Lightweight building envelope, Composite timber wall, Vacuum insulation panel, Phase change material, Sustainable buildings

* Corresponding author: E-mail address: ciril.arkar@fs.uni-lj.si (C. Arkar)

1. Introduction

In contemporary buildings, adequate living comfort accompanied by the efficient use of energy is provided to a great extent with the appropriate design of the building envelope, which ensures small heat losses and efficient heat accumulation. According to [Ahmad, Bontemps, Sallée and Quenard \(2006\)](#), [Pajek, Hudobivnik, Kunič and Košir \(2017\)](#) and [Asdrubali, Ferracuti, Lombardi, Guattari, Evangelisti and Grazieschi \(2017\)](#), in modern buildings, lightweight envelopes and construction elements are increasingly used, as well as timber as sustainable construction material. However, the studies also point out that in lightweight building construction, the dynamic thermal properties are less favourable due to insufficient thermal inertia, which can lead to overheating and increased energy demand for cooling and heating. The parameters of thermal comfort are even more deteriorated if possible future climate scenarios are considered ([Taranto Rodrigues, Gillott & Tetlow, 2013](#)).

The dynamic thermal properties of lightweight building envelope elements can be improved by increasing heat capacity. As can be seen from the overview presented by [Soares, Santos, Gervásio, Costa and da Silva \(2017\)](#), phase change materials (PCM) are most often used for increasing the heat capacity. In this way, increased thermal storage capacity, improved thermal resistance, and higher utilisation of solar energy and energy of the environment are achieved. Improved thermal comfort and decreased heating and cooling load is another advantage of PCM thermal mass. From a detailed overview of research, prepared by [Mavrigiannaki and Ampatzi \(2016\)](#), it can be seen that the largest number of studies analysed PCM integrated into walls, where PCM is the most common within gypsum board. [Pajek et al. \(2017\)](#) analysed the thermal response of different lightweight building constructions for different climate conditions and proved that lightweight construction with PCM had improved thermal response, which however depends on selected PCM melting temperature and climatic conditions. [El Mankibi, Zhai, Al-Saadi and Zoubir \(2015\)](#) present a parametric study of PCM-enhanced walls. The study shows that the highest reduction of peak and seasonal heating and cooling load is achieved when the PCM layer is located on the interior side of construction and that PCM enhanced walls can prevent thermal discomfort. Because of that applications and studies with PCM layers in heavyweight building construction can also be found ([Mavrigiannaki & Ampatzi, 2016](#); [Osterman, Tyagi, Butala, Rahim & Stritih, 2012](#)). Contemporary non-residential buildings, like shopping centres, sport halls, schools, office buildings and modular buildings are frequently made of prefabricated façade panels, consisting of two steel facings and a thermal insulation core ([Leskovšek & Medved, 2011](#)). [Castellón, Medrano, Roca, Cabeza, Navarro, Fernández, Lázaro and Zalba \(2010\)](#) demonstrate the feasibility of using the microencapsulated PCM in prefabricated metal panels to improve the panels' thermal properties and thermal response. PCMs are also used to improve the thermal performance of translucent building envelope elements. [Li, Sun, Zou and Zhang \(2016\)](#) filled one air gap of triple glazing with PCM and reported up to 5.5 °C lower inner surface temperatures and up to 28% lower solar heat gains in comparison to the double- and triple-pane window in the sunny summer days.

However, a particular challenge is posed by thin building envelope elements, which are often found in skeleton frame buildings, where one requirement for opaque parts of the building envelope is that they have a similar thickness as the transparent ones. [Al-Saadi and Zhai \(2015\)](#) studied the thermal performance of a thin lightweight multi-layer wall with PCM on a case study building. Results of the parametric study showed that maximum energy savings are obtained when the PCM layer is located close to the controlled indoor environment. [Ahmad et al. \(2006\)](#) designed wallboard panel with PCM in a polycarbonate panel with an overall wallboard thickness of 53 mm. The wallboard had a vacuum insulation panel (VIP) to increase thermal resistance and improve wallboard efficiency. Experiments conducted on a test cell showed that the amplitude of indoor air temperature variation does not decrease significantly at PCM panel thicknesses above 20 mm. [Favoio, Goia, Perino and Serra \(2016\)](#) combined the PCM and VIP layers in the 'ACTIVE, RESponsive and Solar' façade module, where the VIP is used to thermally disconnect the indoor environment from the air cavity and in which PCM also acted as active thermal energy storage heated by integrated PV modules. VIP panels in multi-layer drywall systems with PCMs also considerably enhanced fire resistance ([Kontogeorgos, Semitelos, Mandilaras & Founti, 2016](#)). Moreover, combined PCM-VIP panel could be beneficial for very thin construction. Development of such a panel, its thermal conductivity, and thermal response to step temperature change were presented by [Li, Chen, Li, Liu, Lu, Zhang and Duan \(2015\)](#).

The increased use of wood and engineered timber products in the building sector has been identified in many market reviews, as presented by [Hildebrandt, Hagemann and Thrän \(2017\)](#). This contributes to more sustainable buildings and to the achievement of the European climate policy targets. Furthermore, the EU policy on Green Public Procurement promotes sustainable and energy efficient building design, construction and renovation. In Slovenia, the Decree on green public procurement

(Official Gazette RS, 2014) specifies the minimal share of wood and timber products, which is set to at least 30% of the volume of installed materials.

The objective of this research was to develop, evaluate, and optimize the dynamic thermal properties of a thin, lightweight composite timber façade wall. A composite timber wall consists of a high volume share of timber with additional commercially available advanced materials: VIP and PCM panels. The thermal response of the composite timber wall was evaluated experimentally and numerically under dynamic outdoor and indoor boundary conditions and compared to the solid (laminated) timber wall of the same thicknesses. The composite timber wall was optimised so as to achieve significantly improved dynamic thermal properties and to meet the energy efficiency requirements of nearly-zero energy buildings. This optimisation includes the determination of the optimal position of VIP and PCM panels within composite timber walls with regard to specified dynamic boundary conditions.

2. Thin, lightweight composite timber wall design and heat transfer mathematical model

2.1. Design of lightweight composite timber façade wall

In the construction of modern residential and commercial buildings (Fig. 1), lightweight construction is increasingly being used. Examples of such elements are metal façade panels and large prefabricated walls that include transparent and opaque parts, which enables quick installation and the optimization of construction costs. It is often desired that opaque parts of such building envelope constructions have thicknesses that are comparable to the thickness of transparent parts of construction elements (built-in windows). These opaque parts of the construction elements are usually multi-layered and thin, while their U-value corresponds to the national energy efficiency requirements applicable to windows and doors but not to external walls.



Fig. 1. Buildings made of thin, lightweight building envelope elements: metal façade (left), thin prefabricated opaque/transparent walls (middle), mobile homes (right).

The aim of the study was to design thin opaque building envelope elements in such a way that their design thermal transmittance (U-value) would meet the requirements for the external wall and would have the dynamic thermal properties similar to the dynamic properties of brick or concrete building construction elements (i.e. a time shift of a periodic heat wave propagation greater than 6 hours).

Since legislation promotes the increased use of sustainable materials, such a thin building envelope element was designed as a composite timber wall with two additional thin layers to increase thermal resistance and heat accumulation ability.

To achieve this, advanced technologies from the field of thermal insulation and increase of thermal capacity had to be used. For increasing the thermal resistance, a commercially available product, TURVAC Si™ Vacuum Insulation Panels (Turna d.o.o., 2017) was used. The TURVAC Si VIP has a fumed silica core material and service life of over 40 years. Reported thermal conductivity can be as low as 0.0045 W/mK. To increase thermal capacity, commercially available PCM was also used. There are several suitable PCMs, that can be found in Mavrigiannaki and Ampatzi (2016) and Saffari, de Gracia, Ushak and Cabeza (2017). DuPont™ Energain® (DuPont Energain, 2017) was selected, which contains

form-stable microencapsulated PCM: a polymer-paraffin compound in aluminium-laminated panels. The latent heat capacity of compound PCM is approximately 70 kJ/kg, and the weight of a 5.2 mm-thick panel is 4.5 kg/m². Fig. 2 shows a schematic of the lightweight composite timber façade wall. PCM and VIP panels were integrated between layers of timber. The position and thickness of VIP and PCM layers will be optimised according to thermal transmittance and dynamic thermal response.

2.2. Numerical heat transfer model of a composite timber wall

Transient heat transfer within a multi-layer wall is assumed to be one-dimensional. When using numerical tools, most commonly partial differential heat diffusion equation with corresponding boundary and initial conditions were solved numerically. In this study, the energy balance method was used to form a set of finite-difference equations for the composite timber wall. Spatial discretisation is performed based on the thermal resistance of each layer, considering the half width of the outer and inner surface node, in order to achieve appropriate accuracy, which was additionally tested by using a mesh-refining technique.

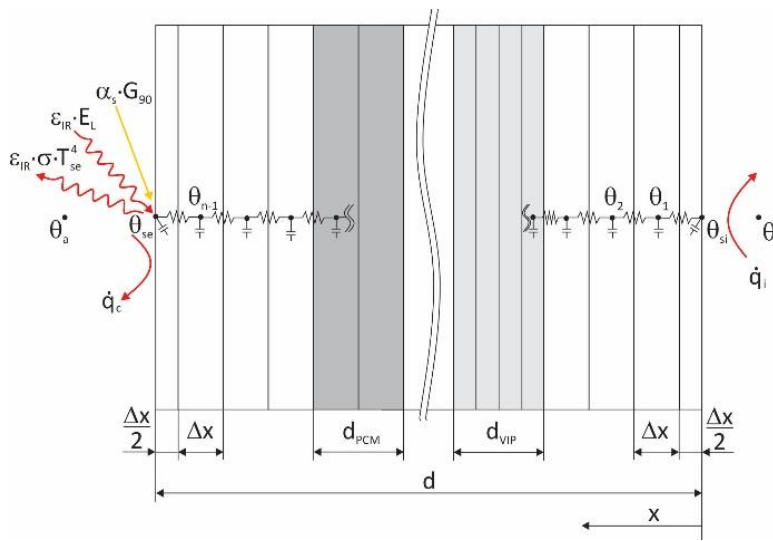


Fig. 2. Schematic of the nodal network and heat fluxes considered in the mathematical model of a thin composite timber façade wall with PCM and VIP layer.

Heat fluxes considered in the model are presented in Fig. 2. The energy balance equations for the inner and outer surface node, having θ_{si} and θ_{se} surface temperatures, are the following:

$$(\rho \cdot c_p) \cdot \frac{\Delta x}{2} \cdot \frac{d\theta_{si}}{dt} = -\frac{k}{\Delta x} \cdot (\theta_{si} - \theta_i) + h_i \cdot (\theta_{si} - \theta_i) \quad (1)$$

$$(\rho \cdot c_p) \cdot \frac{\Delta x}{2} \cdot \frac{d\theta_{se}}{dt} = \alpha_s \cdot G_{90} + \varepsilon_{IR} \cdot E_L - \varepsilon_{IR} \cdot \sigma \cdot T_{se}^4 - h_e \cdot (\theta_{se} - \theta_a) - \frac{k}{\Delta x} \cdot (\theta_{se} - \theta_{n-1}) \quad (2)$$

where G_{90} is solar radiation on the outer surface plane, α_s is absorptivity of solar radiation, ε_{IR} is emissivity of long-wave radiation and E_L is downward long-wave radiation, measured using a pyrgeometer. If measured data are not available, this heat flux can be calculated as presented by Šuklje, Medved and Arkar (2016). Convective heat transfer coefficient on outer surface h_e was determined using correlations proposed by Palyvos (2008): $h_e = 7.4 + 4 \cdot u_w$ for windward conditions and $h_e = 4.2 + 3.5 \cdot u_w$ for leeward conditions, u_w is the wind speed. The inner surface heat transfer coefficient h_i accounts for convective and radiation heat transfer. In numerical analyses, it was assumed to be 7.7 W/m²K, according to EN ISO 6946:2007. Energy balance equations for the interior

nodes consider heat conduction and heat accumulation, neglecting thermal contact resistance between layers of the composite timber wall. The thermo-physical properties are assumed to be constant except for the PCM layer, for which apparent specific heat is determined as explained by [Arkar and Medved \(2005\)](#) and using data presented by [Eddhahak-Ouni, Colin and Bruneau \(2013\)](#). From the results of the DSC measurements, latent heat of phase change was estimated to be 72 kJ/kg. From the product specification, a peak melting temperature is 21.7 °C and the thermal conductivity is 0.18 W/mK when solid and 0.14 W/mK when in a liquid state. The apparent specific heat of Energain PCM was approximated using two polynomial equations:

$$\begin{aligned} 10^{\circ}\text{C} < \theta_{PCM} < 22^{\circ}\text{C}: \quad c_{p,app} &= 13500 - 2194 \cdot \theta_{PCM} + 147.3 \cdot \theta_{PCM}^2 - 1.86 \cdot \theta_{PCM}^3 \\ 22^{\circ}\text{C} \leq \theta_{PCM} < 26^{\circ}\text{C}: \quad c_{p,app} &= 2618944 - 298007 \cdot \theta_{PCM} + 11325.4 \cdot \theta_{PCM}^2 - 143.5 \cdot \theta_{PCM}^3 \end{aligned} \quad (3)$$

Outside this temperature range, $c_{p,app}$ was set to 4500 J/kgK.

The set of implicit finite-difference equations were solved using the matrix inversion method within an MS Excel environment. Spatial discretisation of the timber, VIP, and PCM layers was performed based on the thermal resistance of each layer; 26 divisions were used, considering half width of the outer and inner surface node for greater accuracy of the numerical solution. A time step of 30 s was used for model validation as well as in numerical analysis. In-situ experiments were conducted to validate the developed model.

3. Experimental setup and model validation

The experimental setup was designed in a way to enable parallel in-situ measurement of two different compositions of lightweight, thin building envelope elements. One was a laminated timber wall (*ltw*) and the second was a composite timber wall with VIP and PCM layer (*ctw*). The thicknesses of laminated timber and composite timber walls both equalled 66 mm. The laminated timber wall consisted of six timber plates with equal thermo-physical properties, presented in Table 1. The composite timber wall consisted of timber plates, a 6 mm-thick VIP panel and a 10 mm-thick PCM panel (two layers of DuPont Energain PCM) as presented in Fig. 3. Thermo-physical properties of these materials are presented in Table 1. The PCM panel was located on the inner side after the 10 mm timber lining, while the VIP panel was placed after the outer timber lining (also 10 mm thick). The composite timber wall was designed in such a way that the positions of VIP and PCM panels could be changed. Both, laminated and composite timber wall, were mounted on a south-oriented façade of an office building. Additional side thermal insulation was provided to minimise the thermal bridge effect. The experiment was performed during operation of the building.

Table 1

Materials and thermo-physical properties of laminated timber and composite timber façade wall

	ρ (kg/m ³)	k (W/mK)	c_p (J/kgK)
Wood – timber plates	450	0.14	2000
VIP panel (Turna d.o.o. TURVAC Si™)	200	0.0045	400
PCM panel (DuPont™ Energain®)	865	0.16	$c_{p,app}$ (Eq.3.)

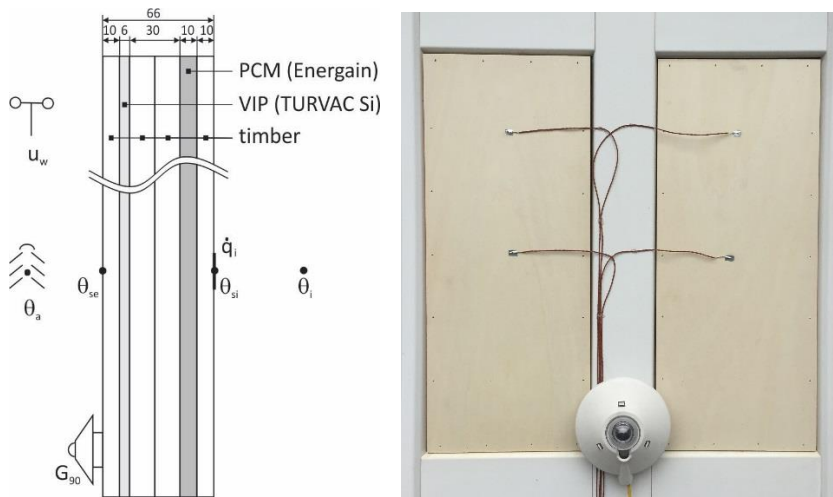


Fig. 3. Schematic of composite timber wall with VIP and PCM layer used in the experiment and the experimental setup (left) and close view (outer side) of comparative in-situ measurements of laminated timber and composite timber wall (right)

Fig. 3 schematically shows the measured variables. Global solar radiation on the vertical plane G_{90} was measured with a Kipp&Zonnen CM11-P pyranometer (measurement uncertainty $\pm 5\%$). Ambient and indoor air temperatures were measured using shielded and well-ventilated K-type thermocouples ($\pm 0.5\text{ }^{\circ}\text{C}$). Calibrated thermocouples were also used for measurements of the wall's surface temperatures ($\pm 0.25\text{ }^{\circ}\text{C}$). The uncertainty of wind velocity measurements was estimated to $\pm 10\%$, as it was not measured in the close vicinity of the installed walls.

In-situ measurements of laminated timber wall and composite timber wall were performed at real outdoor and indoor boundary conditions. In Fig. 4 ambient (θ_a) and indoor (θ_i) air temperatures, solar radiation (G_{90}) and inner surface heat fluxes (\dot{q}_i) measurement results are presented for 6 days with spring weather conditions. Negative inner surface heat flux in Fig. 4 indicate heat flux toward ambient (heat losses) and positive toward interior (heat gains). Calculated daily solar irradiation (H_{90}) on a unit area of vertical measured walls and amplitude (A_{θ}) of ambient and indoor air temperature variation is also presented. The amplitude of indoor air temperature variation corresponds to category B of thermal comfort requirements specified in the [EN ISO 7730:2005](#) standard. The amplitude was higher in days with higher daily solar irradiation because shading devices on windows were not used. The highest heat losses of laminated timber wall could be observed in the night-time, in which (from 18.00 to 7.00 next day) heat losses of the measured composite timber wall were 38% to 59% lower than heat losses of laminated timber wall. Night-time heat losses were lower due to VIP thermal insulation, which reduces the wall U-value and due to the PCM layer, which increases the ability of heat accumulation of the composite wall. The time lag of inner surface peak heat flux (\dot{q}_i) in the range from 3 h to 4 h can be observed from the presented results.

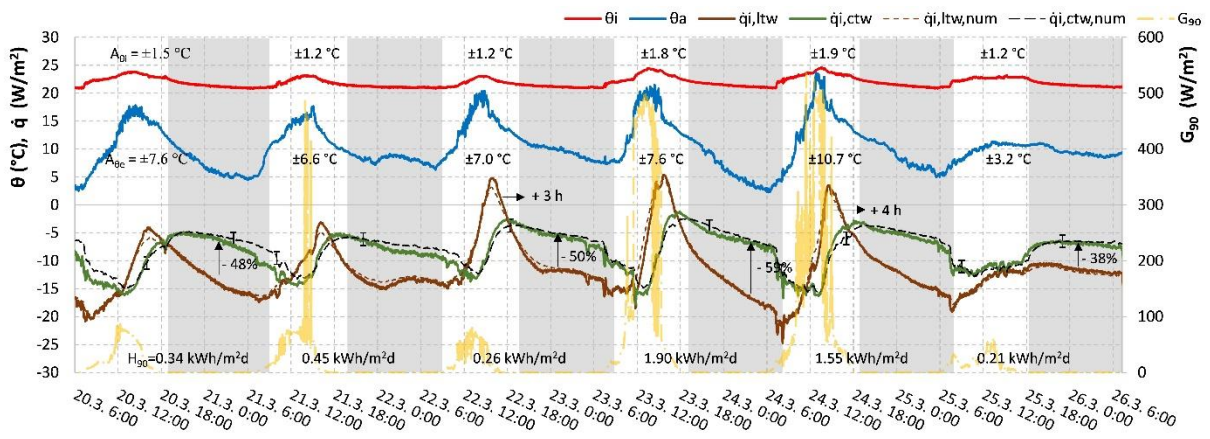


Fig. 4. In-situ measured solar radiation, air temperatures and inner surface heat flux for laminated timber (*ltw*) and composite timber wall (*ctw*) and calculated heat flux of composite timber wall ($d_{VIP} = 6 \text{ mm}$, $d_{PCM} = 10 \text{ mm}$).

A numerical model of the composite timber wall, which was presented in section 2.2., was validated using the presented in-situ measurement results. The absorptivity of solar radiation (α_s) of the outer timber lining was set to 0.5 and emissivity (ε_{IR}) to 0.92, based on a comparison of measured and calculated outer surface temperatures. The inner surface heat transfer coefficient h_i was determined for each time step from the measured air and inner surface temperature and measured heat flux. The convective heat transfer coefficient on outer surface h_e was determined from measured wind velocities and using the presented correlation for leeward conditions. Downward long-wave radiation E_L from the sky and adjacent surfaces was calculated according to the cloud coverage factor and taking into consideration that surrounding surfaces, encountered in radiative heat exchange, have the same temperature as the ambient air. Calculated inner surface heat flux for laminated and composite timber wall is presented in Fig. 4 with a dashed line. Good agreement between the calculated and measured inner surface heat flux can be observed, except for the composite timber wall at the end of the first night shown (21.3.: 2:00–12:00), which can be associated with the set initial conditions. Average deviations between measured and calculated inner surface heat flux in the presented 6-day period are 0.25 W/m^2 for laminated and 0.35 W/m^2 for the composite timber wall. The maximum observed deviations are 5.7 W/m^2 for the laminated and 5.4 W/m^2 for the composite timber wall, observed at the period of the quick change of measured heat flux due to change in the inner surface convective heat transfer (draught). Nevertheless, the uncertainty of measured values (G_{90} , θ_i , θ_a , u_w) and calculated and estimated values (E_L , α_s , ε_{IR}) influence the obtained numerical results. These effects were investigated for the composite timber wall using the Monte-Carlo method (Herrador, Asuero & Gonzalez, 2015, Šuklje, Medved & Arkar, 2016) for the propagation of distributions. A rectangular distribution of random numbers within an uncertainty range was associated with each variable. Stated measurement uncertainties were used in the analysis. For the calculated and estimated values (E_L , α_s , ε_{IR}) the uncertainty was set to $\pm 10\%$. The results of the analysis are shown in Fig. 4 as the uncertainty intervals for selected points.

4. Composite timber façade wall design optimization and performance analysis

The validated transient one-dimensional heat transfer numerical model was used for composite timber wall optimization. Optimization was performed by analysis of the influence of the position of VIP and PCM layers within the composite timber wall on selected performance metrics. A discrete number of different positions of VIP and PCM layers was analysed. Used boundary conditions and performance metrics are presented next. In the analysis, dynamic boundary conditions were considered, as

presented in Fig. 5. Solar radiation on the vertical surface of the composite timber wall was approximated using the Gaussian function, considering daily solar irradiation (H_{90}) of 0.5, 1.5, and 2.5 kWh/m²day. Ambient and indoor air temperatures were approximated using the cosine trigonometric function, considering the same average daily temperature of 5 °C for ambient air and 22 °C for indoor air. The amplitude of ambient air temperature variation (A_{θ_a}) was set to 2 °C, 4 °C, and 6 °C, the highest amplitude being considered in the day with the highest daily solar irradiation. For the indoor air, the amplitude of temperature variation (A_{θ_i}) of 1 °C, 2 °C and 3 °C was used. That corresponds to categories A, B, and C of the design criteria for operative temperature in the office buildings in the heating season (EN ISO 7730:2005). These indoor air dynamic boundary conditions were considered for all three different dynamic conditions on the outer side.

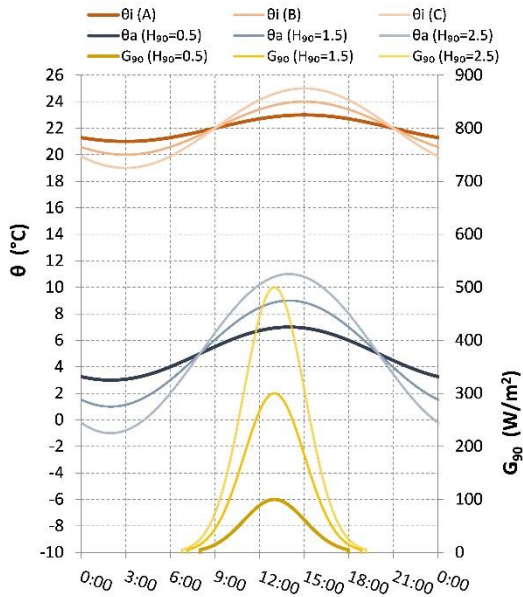


Fig. 5. Indoor and outdoor temperature and solar radiation boundary conditions adopted for analysis

Performance parameters that were adopted for performance analysis were selected so as to be easily recognized by building designers and experts. The thermal transmittance (U-value) was calculated at steady-state conditions as defined in EN ISO 6946:2007 for the laminated and composite timber façade wall and compared with an effective thermal transmittance U_{eff} . The U_{eff} was determined from the numerical results, considering the specified dynamic boundary conditions and with the numerical model determined inner surface heat flux. The U_{eff} value was calculated in the same way as by in-situ measurements:

$$U_{eff} = \frac{\int_0^{24h} \Phi_i \cdot d\tau}{\int_0^{24h} (\theta_a - \theta_i) \cdot d\tau} = \frac{\sum_{j=1}^{n=2880} \Phi_i}{\sum_{j=1}^{n=2880} (\theta_a - \theta_i)} \quad (4)$$

where n is 2880 as the 30 s time interval ($d\tau$) was used. As in numerical calculations, several days with the same boundary conditions were used for each run, the U_{eff} value was determined from numerical results for the last 24 h period. By comparing U-value and U_{eff} value, the influence of absorbed daily solar irradiation on the decrease of façade wall daily heat losses can be estimated. The dynamic performance of the composite timber façade wall was evaluated with two additional indicators. Following the obtained experimental results and based on knowledge of buildings thermal

response and energy need for heating, the heat losses were evaluated in the period of the day when the indoor air temperature was not above the set-point temperature due to the solar and internal heat gains. For easier comparison of heat losses, the period from 19:00 in the evening to 8:00 in the morning of the next day was selected for the calculation of night-time heat losses. A commonly used parameter for evaluation of dynamic properties of building construction and its ‘thermal mass’ is a time lag of 24 h periodic heat wave propagation through the building construction (Kontoleon & Bikas, 2007), which is defined as the time difference between the maximum daily external and internal surface temperatures. In the case of non-sinusoidal periodic boundary conditions, Mazzeo, Oliveti and Arcuri (2016) proposed that the time lag be calculated concerning the peak heat flux on the outer and inner surfaces of building construction:

$$\Delta t = t_{\phi_{e,\max}} - t_{\phi_{i,\max}} \quad (5)$$

where $\phi_{e,\max}$ is the peak heat flux toward the interior (maximum heat gains), while $\phi_{i,\max}$ is the peak heat flux toward the interior (max. heat gains) or the minimum heat flux toward ambient (min. heat losses).

The analysis was performed for a laminate timber and composite timber façade wall with a thickness of 68 mm, which is the most common thickness of windows and doors. The thermo-physical properties of wood, VIP, and PCM materials were the same as specified in Table 1. On the outer boundary conditions, $\alpha_s = 0.8$ and $\varepsilon_{IR} = 0.9$ were used, which corresponds to the dark wood protection coating. Convective heat transfer was determined using constant heat transfer coefficients $h_i = 7.7 \text{ W/m}^2\text{K}$ and $h_e = 17.7 \text{ W/m}^2\text{K}$.

The laminated timber façade wall with a thickness of 68 mm has a U-value of $1.525 \text{ W/m}^2\text{K}$. This is higher than the maximum allowed value for windows and doors in most EU countries. By considering different specified outer and inner side dynamic boundary conditions, the U_{eff} value between $1.47 \text{ W/m}^2\text{K}$ and $1.34 \text{ W/m}^2\text{K}$ was obtained (Fig. 6a).

To reduce the U-value, the VIP panel was added to form the composite timber wall (ctw_{VIP}) of the same thickness ($d = 68 \text{ mm}$). The selected thickness of VIP panel was 10 mm, which is the smallest thickness, according to the product specification. The U-value of such a composite timber façade wall equals $0.357 \text{ W/m}^2\text{K}$. The position of the VIP panel within the composite wall has no influence on the composite wall U-value; however, it affects the U_{eff} value due to the dynamic boundary conditions (Fig. 6a). Results of this analysis are presented in Fig. 6b for the two different daily solar irradiations. The relative position of the VIP panel within the composite timber wall is shown (x/d), with x being the distance of the middle of the VIP panel from the composite wall’s inner surface.

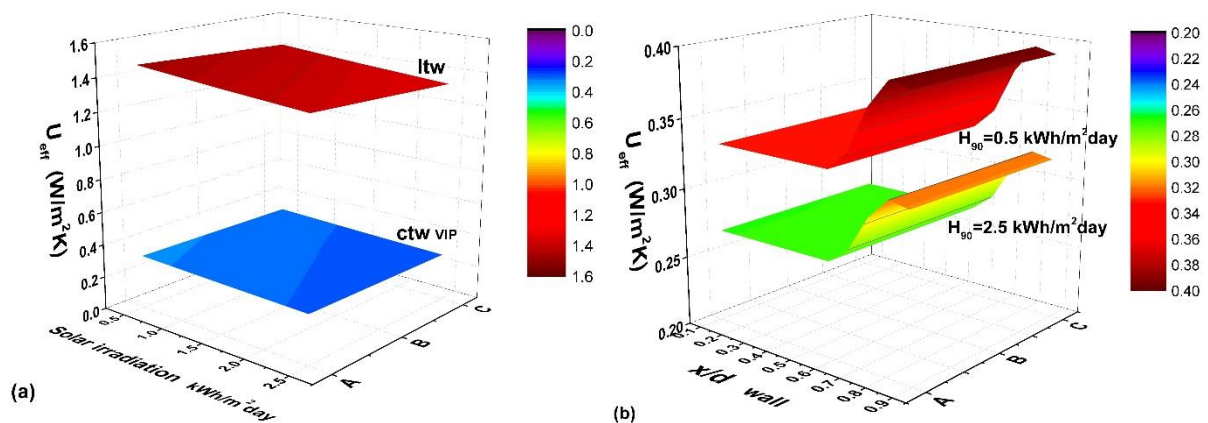


Fig. 6. U_{eff} values of laminated and composite timber wall with integrated VIP panel (ctw_{VIP}) according to outdoor and indoor dynamic boundary conditions (a) and U_{eff} values of ctw_{VIP} according to the relative position of VIP panel in the composite wall at different boundary conditions (b)

The results (Fig. 6.) showed that the VIP panel should be placed on the inner half of the composite timber wall to obtain the lowest U_{eff} value. The U_{eff} value depends on daily solar irradiation on the wall surface, being 0.33 W/m²K and 0.267 W/m²K at H_{90} of 0.5 kWh/m²day and 2.5 kWh/m²day respectively. This represents 8% to 25% decrease in the U_{eff} value compared to the ctw_{VIP} design U-value. Results also showed that dynamic indoor conditions have a minor influence on U_{eff} value, while dynamic outdoor conditions have a large influence on the thermal properties of such composite timber walls.

In the next step, the composite timber façade wall thermal mass was increased with the integration of a PCM layer. Based on experimental results and considering the thickness of thin composite timber wall two Energain plates were added with total thickness $d_{PCM} = 10$ mm. Composite timber wall was designed with VIP, and PCM layers placed one next to another, as this is most convenient. Two options were analysed; a PCM layer is facing indoor and VIP layer toward ambient (ctw_{PCM_i, VIP_e}) and VIP layer facing toward indoor and PCM layer toward ambient (ctw_{VIP_i, PCM_e}). The $ctw_{VIP, PCM}$ U-value could be considered the same as the U-value of ctw_{VIP} , because the thermal conductivity of the PCM layer is similar to the thermal conductivity of wood (Table 1). The calculated U_{eff} values are also similar, as presented in Fig. 7 for the case of daily solar irradiation on the outer surface of 2.5 kWh/m²day. The optimal U_{eff} values differ for 0.01 W/m²K. Furthermore, from these results, it can be concluded that the VIP/PCM layer should be located on the inner half of the composite timber wall.

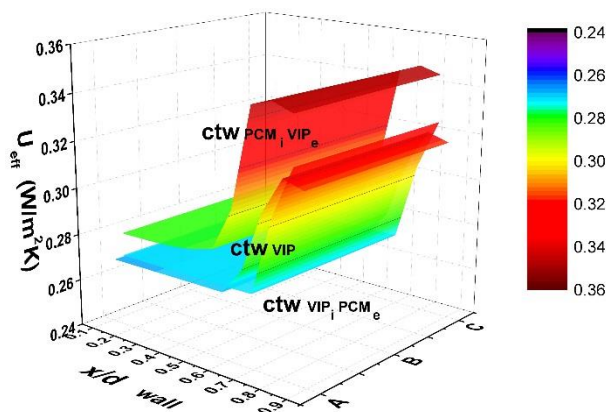


Fig. 7. U_{eff} values of composite timber walls with integrated VIP panel and integrated VIP/PCM panels according to the relative position of VIP or VIP/PCM panel in the composite wall and different indoor boundary conditions; $H_{90} = 2.5$ kWh/m²day.

Energy use for heating and cooling, as well as indoor thermal comfort conditions, are largely influenced by the building's construction dynamic properties, which were next evaluated for different composite timber façade walls. As stated in Favoino, Goia, Perino & Serra (2016), during the daytime, heating demand in energy efficient office buildings is low or zero due to solar and internal gains, so night-time heat losses (q_{night}) were selected as a parameter for evaluation of the dynamic properties. The results of the analysis are presented in Fig. 8, where positive values indicate heat losses and negative heat gains. From the results, it could be seen that night-time heat losses also depend on indoor dynamic

boundary conditions, which was not the case for U_{eff} value. Moreover, the most favourable position of VIP panel or VIP/PCM panel within the composite timber façade wall is different and depends on indoor boundary conditions. For the ctw_{VIP} and ctw_{VIP_i,PCM_e} the most favourable position of VIP or VIP/PCM panel on $x/d = 1/2$ is at category A and $x/d = 2/3$ at category C of indoor temperature conditions. For the ctw_{PCM_i,VIP_e} the PCM/VIP panel should be located at $x/d \leq 1/3$. The night-time heat losses of the ctw_{VIP} wall with VIP panel on optimal position ranges from 69.8 Wh/m²day (category A) to 43.8 Wh/m²day (category C). Heat losses of the ctw_{VIP_i,PCM_e} wall are approximately 10 Wh/m²day lower than at ctw_{VIP} wall. The most favourable conditions are observed for the ctw_{PCM_i,VIP_e} wall, with PCM facing indoor. At category A of dynamic indoor conditions, the lowest night-time heat losses are 38.2 Wh/m²day. Meanwhile, at category C conditions, night-time heat gains of 16 Wh/m²day were observed. From the presented results, it is clear that when both VIP and PCM panels are used, the PCM panel should be facing the inner side to improve the dynamic thermal response. As the actual phase change temperature range of Energain PCM panel was used in the analysis, one can conclude that only part of PCM latent heat was exploited for heat accumulation, the share being larger at larger amplitudes of indoor air temperature variations (category C). For the comparison, which is not shown in Fig. 8, the night-time heat losses of laminated timber wall are in the range between 325 Wh/m²day and 360 Wh/m²day. Thus, night-time heat losses of ctw_{VIP} are 80-87% lower and of ctw_{PCM_i,VIP_e} at least 90% lower than heat losses of ltw .

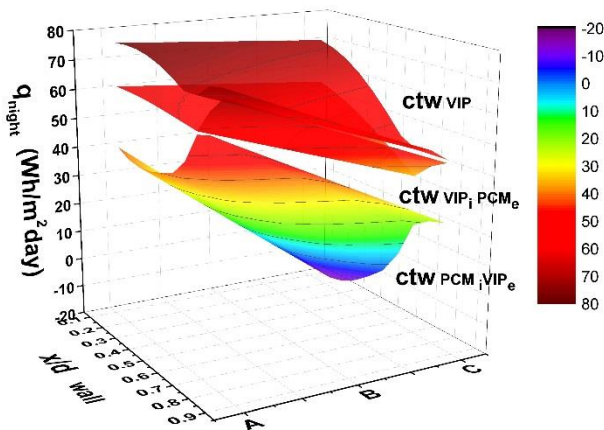


Fig. 8. Composite timber façade walls' heat losses in the night-time period (from 19:00 until 8:00) according to the relative position of VIP or VIP/PCM panel in the composite wall and different indoor boundary conditions; $H_{90} = 2.5$ kWh/m²day.

The time lag of periodic heat wave propagation through the composite timber façade walls was determined considering the optimal position of VIP and PCM/VIP panels within the composite timber wall. The time lag (Fig. 9) between 2 h and 3.5 h can be expected for the laminated timber wall, being the highest at low daily solar irradiation ($H_{90} = 0.5$ kWh/m²day) and at a high amplitude of indoor air temperature variation ($A_{\theta_i} = 3$ °C). The time lag of composite timber wall with VIP panel ranges between 3 h and 10 h. The highest time lag, between 9 h and 12 h, was achieved for ctw_{PCM_i,VIP_e} , which is the most favourable in term of peak heat load and heat loss reduction of the building. Further improvements of the composite timber façade wall, especially the design U-value, are possible by using the higher thickness of the VIP panel.

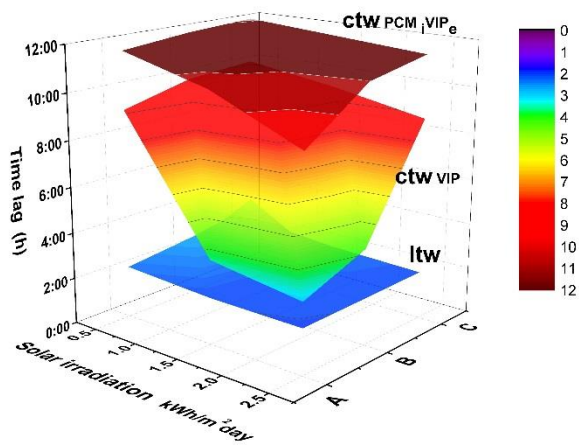


Fig. 9. Time lag of periodic heat wave propagation for laminated timber wall and for composite timber façade walls with VIP and VIP/PCM panels at optimal location within ctw .

5. Conclusions

This paper presents the development of sustainable and energy efficient alternatives to thin, lightweight opaque façade elements, such as prefabricated metal façade panels, prefabricated walls with thin opaque parapets and doors, and façade walls for mobile and modular buildings. The high share of sustainable, timber material was ensured by selecting advanced technologies to improve the thermal properties of the developed thin composite timber façade wall. Commercially available advanced products were used: VIP Turna, TURVAC Si, and PCM DuPont Energain. Performed parallel in-situ measurements of laminated timber and composite timber façade wall showed the improved thermal response of the composite wall, as well as the dynamic boundary conditions on both planes, which were considered in the performed numerical research.

A transient heat transfer numerical model of a composite wall was developed and validated. In the numerical analysis, a composite timber wall with a thickness of 68 mm with integrated PCM and VIP panels, both with thicknesses of 10 mm, was optimised to ensure optimal thermal properties and thermal response at dynamic boundary conditions. The performed analysis revealed that PCM and VIP panels should be placed in the inner third of the composite wall width, with PCM facing inside. The composite wall U-value, determined at steady-state conditions, of $0.358 \text{ W/m}^2\text{K}$ was achieved; meanwhile, the U_{eff} value, which takes into account the dynamic boundary conditions, reduced below $0.33 \text{ W/m}^2\text{K}$. A further reduction of U-value, in case it should comply with national regulations, would require a higher thickness of the VIP layer. The dynamic thermal response of the composite timber wall was evaluated with the night-time heat losses. The analysis showed that night-time heat losses of the composite wall are at least 90% lower than with the laminated timber wall, and can turn to heat gains in case of daily solar irradiation higher than $2 \text{ kWh/m}^2\text{day}$. Above all, the time lag of heat wave propagation, which was between 9 h and 12 h for the optimal composition of the composite timber wall, indicates the improved ability of heat accumulation and dynamic thermal response, which is similar to the thermal response of brick or concrete walls.

Acknowledgments

The authors acknowledge the financial support from the Slovenian Research Agency (research core funding No. P2-0223 (C)). The authors are grateful to Turna d.o.o. and DuPont de Nemours International S.A., Representative Office Slovenia for supporting the research by supplying some of the components of the composite timber façade wall. This work was also supported by the European

Regional Development Fund, Research and development programmes (TRL 3-6), Programme: 'Sustainable and innovative construction of smart buildings – TIGR4smart' (C3330-16-529003).

References

Ahmad, M., Bontemps, A., Sallée, H., & Quenard, D. (2006). Thermal testing and numerical simulation of a prototype cell using light wallboards coupling vacuum isolation panels and phase change material. *Energy and Buildings*, 38 673–681. <http://dx.doi.org/10.1016/j.enbuild.2005.11.002>

Al-Saadi, S.N., & Zhai, Z.J. (2015). A new validated TRNSYS module for simulating latent heat storage walls. *Energy and Buildings*, 109, 274–290. <http://dx.doi.org/10.1016/j.enbuild.2015.10.013>

Arkar, C. & Medved, S. (2005). Influence of accuracy of thermal property data of a phase change material on the result of a numerical model of a packed bed latent heat storage with spheres. *Thermochimica Acta*, 438, 192–201. <https://doi.org/10.1016/j.tca.2005.08.032>

Asdrubali, F., Ferracuti, B., Lombardi, L., Guattari, C., Evangelisti, L., & Grazieschi, G. (2017). A review of structural, thermo-physical, acoustical, and environmental properties of wooden materials for building applications. *Building and Environment*, 114, 307–332. <http://dx.doi.org/10.1016/j.buildenv.2016.12.033>

Castellón, C., Medrano, M., Roca, J., Cabeza, L.F., Navarro, M.E., Fernández, A.I., Lázaro, A., & Zalba, B. (2010). Effect of microencapsulated phase change material in sandwich panels. *Renewable Energy*, 35, 2370–2374. <https://doi.org/10.1016/j.renene.2010.03.030>

Decree on green public procurement, Official Gazette of the Republic of Slovenia, no. 89/14. (2014). <http://www.pisrs.si/Pis.web/pregledPredpisa?id=URED5194#> Accessed 12.08.17

DuPont Energain. http://www.cse.fraunhofer.org/hs-fs/hub/55819/file-14736951-pdf/docs/energain_flyer.pdf Accessed 02.02.17

Eddhahak-Ouni, A., Colin, J., & Bruneau, D. (2013). On an experimental innovative setup for the macro scale thermal analysis of materials: Application to the Phase Change Material (PCM) wallboards. *Energy and Buildings*, 64, 231–238. <http://dx.doi.org/10.1016/j.enbuild.2013.05.008>

El Mankibi, M., Zhai, Z.J., Al-Saadi, S.N. & Zoubir, A. (2015). Numerical modeling of thermal behaviors of active multi-layer living wall. *Energy and Buildings*, 106, 96–110. <http://dx.doi.org/10.1016/j.enbuild.2015.06.084>

EN ISO 6946:2007. Building components and building elements - Thermal resistance and thermal transmittance - Calculation method (ISO 6946:2007)

EN ISO 7730: 2005. Ergonomics of the thermal environment - Analytical determination and interpretation of thermal comfort using calculation of the PMV and PPD indices and local thermal comfort criteria (ISO 7730:2005)

Favoino, F., Goia, F., Perino, M., & Serra, V. (2016). Experimental analysis of the energy performance of an ACTIVE, RESPONSIVE and SOLAR (ACTRESS) façade module. *Solar Energy*, 133, 226–248. <http://dx.doi.org/10.1016/j.solener.2016.03.044>

Herrador, M. A., Asuero, A. G., & Gonzalez, A. G. (2015). Estimation of the uncertainty of indirect measurements from the propagation of distributions by using the Monte-Carlo method: An overview. *Chemometrics and Intelligent Laboratory Systems*, 79, 115–122. <https://doi.org/10.1016/j.chemolab.2005.04.010>

- Hildebrandt, J., Hagemann, N., & Thrän, D. (2017). The contribution of wood-based construction materials for leveraging a low carbon building sector in Europe. *Sustainable Cities and Society*, 34, 405–418. <http://dx.doi.org/10.1016/j.scs.2017.06.013>
- Kontogeorgos, D.A., Semitelos, G.K., Mandilaras, I.D., & Founti, M.A. (2016). Experimental investigation of the fire resistance of multi-layer drywall systems incorporating Vacuum Insulation Panels and Phase Change Materials. *Fire Safety Journal*, 81, 8–16. <http://dx.doi.org/10.1016/j.firesaf.2016.01.012>
- Kontoleon, K.J., & Bikas, D.K. (2007). The effect of south wall's outdoor absorption coefficient on time lag, decrement factor and temperature variations. *Energy and Buildings*, 39, 1011–1018. <http://dx.doi.org/10.1016/j.enbuild.2006.11.006>
- Leskovšek, U., & Medved, S. (2011). Heat and moisture transfer in fibrous thermal insulation with tight boundaries and a dynamical boundary temperature. *International Journal of Heat and Mass Transfer*, 54, 4333-4340. <https://doi.org/10.1016/j.ijheatmasstransfer.2011.05.011>
- Li, S., Sun, G., Zou, K., & Zhang, X. (2016). Experimental research on the dynamic thermal performance of a novel triple-pane building window filled with PCM. *Sustainable Cities and Society*, 27, 15–22. <http://dx.doi.org/10.1016/j.scs.2016.08.014>
- Li, X., Chen, H., Li, H., Liu, L., Lu, Z., Zhang, T., & Duan, W.H. (2015). Integration of form-stable paraffin/nanosilica phase change material composites into vacuum insulation panels for thermal energy storage. *Applied Energy*, 159, 601–609. <http://dx.doi.org/10.1016/j.apenergy.2015.09.031>
- Mavrigiannaki, A., & Ampatzi, E. (2016). Latent heat storage in building elements: A systematic review on properties and contextual performance factors. *Renewable and Sustainable Energy Reviews*, 60, 852–866. <http://dx.doi.org/10.1016/j.rser.2016.01.115>
- Mazzeo, D., Oliveti, G., & Arcuri, N. (2016). Influence of internal and external boundary conditions on the decrement factor and time lag heat flux of building walls in steady periodic regime. *Applied Energy*, 164, 509–531. <http://dx.doi.org/10.1016/j.apenergy.2015.11.076>
- Osterman, E., Tyagi, V.V., Butala, V., Rahim, N.A., & Stritih, U. (2012). Review of PCM based cooling technologies for buildings. *Energy and Buildings*, 49, 37–49. <http://dx.doi.org/10.1016/j.enbuild.2012.03.022>
- Pajek, L., Hudobivnik, B., Kunič, R., & Košir, M. (2017). Improving thermal response of lightweight timber building envelopes during cooling season in three European locations. *Journal of Cleaner Production*, 156, 939–952. <http://dx.doi.org/10.1016/j.jclepro.2017.04.098>
- Palyvos, J.A. (2008). A survey of wind convection coefficient correlations for building envelope energy systems' modelling. *Applied Thermal Engineering*, 28, 801–808. <http://dx.doi.org/10.1016/j.applthermaleng.2007.12.005>
- Saffari, M., de Gracia, A., Usha, S., & Cabeza, L.F. (2017). Passive cooling of buildings with phase change materials using whole-building energy simulation tools: A review. *Renewable and Sustainable Energy Reviews*, 80, 1239–1255. <https://doi.org/10.1016/j.rser.2017.05.139>
- Soares, N., Santos, P., Gervásio, H., Costa, J.J., & Simões da Silva, L. (2017). Energy efficiency and thermal performance of lightweight steel-framed (LSF) construction: A review. *Renewable and Sustainable Energy Reviews*, 78, 194–209. <http://dx.doi.org/10.1016/j.rser.2017.04.066>

Šuklje, T., Medved, S., & Arkar, C. (2016). On detailed thermal response modeling of vertical greenery systems as cooling measure for buildings and cities in summer conditions. *Energy*, 115, 1055–1068. <http://dx.doi.org/10.1016/j.energy.2016.08.095>

Taranto Rodrigues, L., Gillott, M., & Tetlow, M. (2013). Summer overheating potential in a low-energy steel frame house in future climate scenarios. *Sustainable Cities and Society*, 7, 1–15. <http://dx.doi.org/10.1016/j.scs.2012.03.004>

Turna d.o.o. (2017). <http://en.turna.si/Programmes/VacuumInsulationPanelsTurvac.aspx> Accessed 05.06.17